Supplementary Information: Transition from Phononic to Geometrical Mie Modes Measured in Single Subwavelength Polar Dielectric Spheres

Loubnan Abou-Hamdan,[†,‡] Laure Coudrat,[†] Sébastien Bidault,[†] Valentina Krachmalnicoff,[†] Riad Haïdar,[‡] Patrick Bouchon,[*,‡] and Yannick De Wilde[*,†]

†*Institut Langevin, ESPCI Paris, PSL University, CNRS, 1 rue Jussieu, F-75005 Paris, France*

‡*DOTA, ONERA, Université Paris-Saclay, F-91123 Palaiseau, France*

E-mail: patrick.bouchon@onera.fr; yannick.dewilde@espci.fr

1 METHODS

1.1 Sample preparation

A 1 μL solution of commercially available microspheres (Sigma Aldrich for SiO_2 and Polysciences for PTFE), of known size, was diluted with 99 μL of solvent (distilled water for SiO_2 and ethanol for PTFE), and sonicated to prevent particle aggregation. The diluted solution was spin-coated on a sample consisting of a 100 nm thick gold layer on top of a silicon (Si) substrate. The sample was viewed using a microscope with a visible objective (x50, Numerical aperture NA=0.55) to determine the positions of single spheres. The spheres were then imaged using a visible cam-

era (Figs. 1 (b)-(e) of the main text, insets) and the thermal radiation of the imaged spheres was characterized using infrared spatial modulation spectroscopy.[1,2]

1.2 Finite element method simulations

1.2.1 Electromagnetic simulations

Finite element method simulations (FEM), using the commercially available software, Comsol Multiphysics, were carried out to calculate the field distributions inside a single sphere in vacuum and the electric field enhancements of spheres in vacuum and on a 100 nm thick gold substrate, in addition to the absorption cross-section of a single sphere on gold. To simulate a single sphere, perfectly matched layers were set for all boundaries. For the sphere on gold, a plane wave port is incident at an angle θ with respect to the normal to the sphere/substrate. The simulation is first run without the sphere, then run again with the sphere so that the field is slightly modified by the presence of the sphere, allowing to take into account the influence of the sub-λ sphere on the large simulation region. For a sphere in vacuum, a plane wave background field was implemented.

The absorption cross-section was calculated by integrating losses of the incident field due to absorption over the volume of the sphere. The computation of the sphere's absorption cross-section on gold is effected for unpolarized light incident at various angles of incidence, $\theta = 10$, 20, and 30^o (see Fig. S2), and the resultant spectra are averaged in order to properly take into account the conic collection of the Cassegrain objective used in the measurements. Field distributions (Fig. 2 (a) and Figs. 3 (b) and (d) of the main text) were obtained by calculating the fields in a slice of the geometry. The simulation span was made twice the wavelength in order to reduce stray reflections off the boundaries and to ensure proper convergence of the simulations.

Data form ref.[3] were used in the simulations for the dielectric function of SiO_2 (Fig. 2 (b), main text), while the dielectric properties of PTFE (Fig. 4 (b), inset, main text) and gold were taken from refs.[4] and,[5] respectively.

1.2.2 Heat transfer simulation

To assess the possibility of a temperature gradient arising in the measured SiO_2 spheres on the hot substrate, we performed FEM simulations of the temperature distribution in our system using the Comsol Multiphysics Heat Transfer module. A 50x50 μm^2 region of the substrate is considered along with a 50 µm thick air layer above it. The substrate is maintained at a temperature of 440 K while we take into account conductive cooling through air and glass. To simulate the poor contact between the sphere and substrate, the sphere is considered to intersect the substrate at a single point. As shown in Fig. S1 (a), we find that, under these conditions, the sphere temperature deviates at maximum by 0.35 K from the substrate temperature.

We note that conduction through the air layer is the main heat transfer channel.[6] We have verified this by suppressing the solid-solid contact so that the sphere is 1 μm above the substrate (Fig. S1 (b)), for which we find that the temperature deviation is still below 1 K. Thus, temperature variations within the sphere are negligible, showing that the assumption that the sphere is thermalized at the temperature of the substrate (440 K) is valid under our experimental conditions.

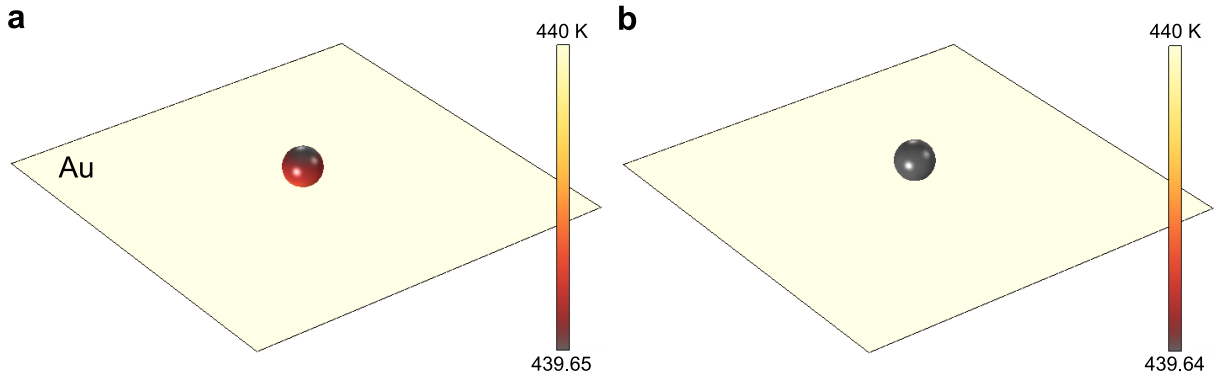

Figure S1: FEM calculations of the temperature distribution in a 2.5 μm radius SiO_2 sphere (a) on and (b) 1 μm above a gold substrate with $T_{substrate} = 440$ K.

2 VIRTUAL MODES AND SPHERE CROSS-SECTIONS

The transverse modes of a polar dielectric sphere of radius r_o and dielectric permittivity ε, illuminated by light of wavelength λ in vacuum, are given by the following equations[7]

$$h_l^{(1)}(\rho_2)[\rho_1 j_l(\rho_1)]' - \varepsilon j_l(\rho_1)[\rho_2 h^{(1)}(\rho_2)]' = 0, \quad \text{(electric modes)} \tag{1}$$

$$h_l^{(1)}(\rho_2)[\rho_1 j_l(\rho_1)]' - j_l(\rho_1)[\rho_2 h^{(1)}(\rho_2)]' = 0, \quad \text{(magnetic modes)} \tag{2}$$

where j_l and $h_l^{(1)}$ are the spherical Bessel and Hankel functions of the first kind, respectively, $\rho_1 = \frac{2\pi r_o}{\lambda}\sqrt{\varepsilon}$, $\rho_2 = \frac{2\pi r_o}{\lambda}$, and $'$ denotes differentiation with respect to the argument of the Bessel functions. The cross-sections of a sphere in free space illuminated by a plane wave can be calculated from Mie theory, and are given by[8]

$$C_{ext} = \frac{\lambda^2}{2\pi}\sum_{l=1}^{\infty}(2l+1)Re(a_l + b_l), \tag{3}$$

$$C_{scat} = \frac{\lambda^2}{2\pi}\sum_{l=1}^{\infty}(2l+1)(|a_l|^2 + |b_l|^2), \tag{4}$$

and

$$C_{abs} = C_{ext} - C_{scat}, \tag{5}$$

where, C_{abs}, C_{scat}, and C_{ext}, are the sphere's absorption, scattering, and extinction cross-sections, respectively. a_l and b_l, are the scattering coefficients, and l is the mode number.

The scattering coefficients can be cast in the following form

$$a_l = \frac{\varepsilon j_l(\rho_1)[\rho_2 j_l(\rho_2)]' - j_l(\rho_2)[\rho_1 j_l(\rho_1)]'}{\varepsilon j_l(\rho_1)[\rho_2 h_l^{(1)}(\rho_2)]' - h_l^{(1)}(\rho_2)[\rho_1 j_l(\rho_1)]'}, \tag{6}$$

$$b_l = \frac{j_l(\rho_1)[\rho_2 j_l(\rho_2)]' - j_l(\rho_2)[\rho_1 j_l(\rho_1)]'}{j_l(\rho_1)[\rho_2 h_l^{(1)}(\rho_2)]' - h_l^{(1)}(\rho_2)[\rho_1 j_l(\rho_1)]'}. \tag{7}$$

By comparing Eqs. 1-2 to Eqs. 6-7, it can be seen immediately that the frequencies of the sphere's transverse virtual modes correspond to that of vanishing denominators of the scattering coefficients a_l and b_l. Thus, the sphere's virtual modes are fully accounted for by the Mie formalism.

3 ANGLE RESOLVED FEM SPECTRA OF A SPHERE ON GOLD

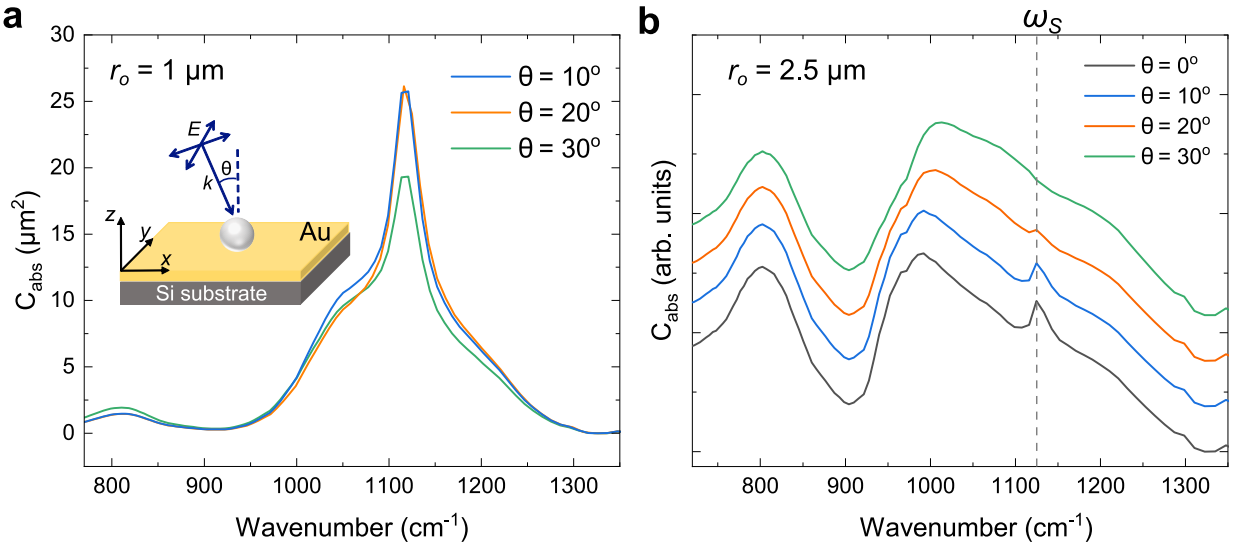

Figure S2: FEM calculations of absorption cross-section (C_{abs}) of an SiO_2 sphere on gold, with (a) $r_o = 1$ μm and (b) $r_o = 2.5$ μm, for unpolarized light incident at various angles θ, as sketched in the inset of panel (a). The curves in panel (b) are shifted vertically for clarity and the dashed vertical line shows the surface mode peak position (ω_S).

References

(1) Li, C.; Krachmalnicoff, V.; Bouchon, P.; Jaeck, J.; Bardou, N.; Haidar, R.; De Wilde, Y. Near-field and far-field thermal emission of an individual patch nanoantenna. *Phys. Rev. Lett.* **2018**,

121, 243901.

(2) Abou-Hamdan, L.; Li, C.; Haidar, R.; Krachmalnicoff, V.; Bouchon, P.; De Wilde, Y. Hybrid modes in a single thermally excited asymmetric dimer antenna. *Opt. Lett.* **2021**, *46*, 981–984.

(3) Palik, E. D. *Handbook of optical constants of solids*; Academic press, 1998; Vol. 3.

(4) Korte, E. H.; Röseler, A. Infrared reststrahlen revisited: commonly disregarded optical details related to $n < 1$. *Anal. Bioanal. Chem.* **2005**, *382*, 1987–1992.

(5) Olmon, R. L.; Slovick, B.; Johnson, T. W.; Shelton, D.; Oh, S.-H.; Boreman, G. D.; Raschke, M. B. Optical dielectric function of gold. *Phys. Rev. B* **2012**, *86*, 235147.

(6) Doumouro, J.; Perros, E.; Dodu, A.; Rahbany, N.; Leprat, D.; Krachmalnicoff, V.; Carminati, R.; Poirier, W.; De Wilde, Y. Quantitative measurement of the thermal contact resistance between a glass microsphere and a plate. *Phys. Rev. Appl.* **2021**, *15*, 014063.

(7) Fuchs, R.; Kliewer, K. Optical modes of vibration in an ionic crystal sphere. *J. Opt. Soc. Am.* **1968**, *58*, 319–330.

(8) Bohren, C. F.; Huffman, D. R. *Absorption and scattering of light by small particles*; John Wiley & Sons, 2008; p 103.